Material Extrusion on an Ultrasonic Air Bed for 3D Printing

2 3 4

1

Keller, Samuel

5 Department of Mechanical Engineering, University of Minnesota 111 Church Street SE, Minneapolis, MN 55455 6

kell2521@umn.edu

7 8 9

Stein, Matthew

10 Department of Mechanical Engineering, University of Minnesota 11 111 Church Street SE, Minneapolis, MN 55455

12 stei1713@umn.edu

13

14 Ilic, Ognjen¹

15 Department of Mechanical Engineering, University of Minnesota

16 111 Church Street SE, Minneapolis, MN 55455

17 ilic@umn.edu

18

19

ABSTRACT

20 21

32

22 Additive manufacturing, such as 3D printing, offers unparalleled opportunities for rapid prototyping of 23 objects, but typically requires simultaneous building of solid supports to minimize deformation and ensure 24 contact with the printing surface. Here, we theoretically and experimentally investigate the concept of 25 material extrusion on an "air bed" – an engineered ultrasonic acoustic field that stabilizes and supports 26 the soft material by contactless radiation pressure force. We study the dynamics of polylactic acid (PLA) 27 filament—a commonly used material in 3D printing—as it interacts with the acoustic potential during 28 extrusion. We develop a numerical radiation pressure model to determine optimal configurations of 29 ultrasonic transducers to generate acoustic fields and conditions for linear printing. We build a concept 30 prototype that integrates an acoustic levitation array with a 3D printer and use this device to demonstrate 31 linear extrusion on an acoustic air bed. Our results indicate that controlled interactions between acoustic

fields and soft materials could offer alternative support mechanisms in additive manufacturing with

¹ ilic@umn.edu

potential benefits such as less material waste, fewer surface defects, and reduced material processing time.

35

33

34

INTRODUCTION

3637

38

39

40

41

42

43

44

45

46

47

48

49

50

51

52

53

54

In additive manufacturing, the creation of complex objects relies on employing effective support structures during the manufacturing process. In processes such as filament extrusion and material jetting, solid supports are often printed simultaneously with the desired object to ensure stability and proper adhesion to a horizontal printer bed. These supports, along with a solid printing bed, can cause significant defects on the surface of objects, lead to warping and deformation, and prevent their detachment from the bed. Additionally, support structures generate considerable material waste, adding to overall manufacturing time and costs. As additive manufacturing technology rapidly evolves, developing more efficient support mechanisms could have a critical impact on 3D printing. These alternatives must account for the complex nature of the soft material filament as it is melted and extruded to ensure minimal deformation as the filament hardens. Here, we study the potential of acoustic radiation pressure fields as a viable mechanism for contactless support of soft materials during extrusion. By directing a tailored acoustic wavefront at the material as it is extruded, we aim to induce a radiative force capable of counteracting the force of gravity as well as spatially stabilizing the material in an acoustic potential. The broader aim is to create a sustainable method to support complex shapes at various angles during printing.

56

57

58

59

60

61

62

63

64

65

66

67

68

69

70

71

72

73

74

75

76

We analyze and demonstrate an ultrasonic acoustic system where contactless acoustic support is integrated into linear 3D printing. Our approach mimics the effect of solid supports in 3D printing by optimally distributing the acoustic radiation force across the filament as it solidifies (Fig. 1). The acoustic radiation force (ARF) [1–5] arises from the momentum change of sound as it scatters from an object and has been used in concepts such as acoustic tweezers and traps [6–16]. Such traps have been used to levitate small animals [17], fluid droplets [18-21], and in chemical analysis and medical devices [22–24]. These acoustic levitators establish symmetrical resonant acoustic traps to levitate single, typically spherical particles. It has been shown that these devices can be used to assemble larger shapes using individual particles as building blocks [25]. Rather than analyzing the concatenation of such particles, here we explore the dynamics for the support of continuous solid manufacturing during soft material extrusion. In doing so, it could be possible to achieve finer surface detail and functionally stronger objects. Acoustic levitation is a compelling platform to study the interaction of acoustic fields with soft materials under extrusion as these devices have the ability to levitate a wide range of materials [26,27], and can be tailored to the specific object being levitated. Our paper is outlined as follows. First, we analyze the stability of a soft-material extruded object (intended to mimic a typical 3D-printer filament) in a controlled ultrasonic acoustic field. Next, we design a full acoustic levitator by evaluating complex acoustic potentials using perturbation theory and finite-element simulations. We then verify the accuracy of our numerical design by constructing a functional device. Finally, we demonstrate that this acoustic levitation device can be

used in conjunction with conventional fused filament fabrication (FFF) 3D printing to achieve the linear trapping of solid and semisolid objects during extrusion.

METHODS

We begin by identifying the pertinent characteristics of existing methods for acoustic levitation. These devices often use a configuration in which the sound source is reflected to create a standing wave [28,29] with nodal traps that support levitation. We tailor the nodal traps by arranging an array of transducers in a concave shape [30]. Focusing the emitted sound waves from either side of the levitation device allows for increased distance between emitters without compromising the maximum radiation force applied. Previous devices using concave transducer arrays have been able to levitate spherical objects [31,32], but often only in the form of spherical caps that focus the field to a small volume in space therefore limiting the shape and size of trapped objects. To address this limitation, we design a custom cylindrical array of transducers capable of levitating linear objects up to the length of the array.

Acoustic System Assembly and Characterization

To design our array, we select the number and the arrangement of transducers with the goal of maximizing output pressure and minimizing the array radius and transducer number . The operating frequency of 40 kHz is selected as this frequency is inaudible to the human ear and gives a maximum trap size of ≈ 4.3 mm ($\lambda/2$). We chose this frequency based on the knowledge that it can generate acoustic traps that are sufficiently large for the purpose of supporting a soft-material filament during

extrusion. Common FDM 3D printers can be equipped with nozzle diameters ranging from 0.1 mm to 2.0 mm. This means that the filament will fit within a single acoustic trap while still having sufficient tolerance for slight offsets in the alignment of the array and extrusion nozzle. The transducer arrays are wired in parallel and driven by a programmed Arduino Nano. A square wave is output and then amplified using a dual h-bridge motor driver. Using this setup, each transducer in the array receives an identical constant signal. A commercial 3D printer (Creality Ender 3) was modified to extrude filament horizontally inside the levitation device, minimizing the downward force applied by the extruder. This printer was chosen as an accessible option that can easily interface with custom user code for full real-time control of each stepper motor.

Modeling and Numerical Analysis

We conduct finite element acoustic simulations in COMSOL Multiphysics to predict the behavior and optimize the performance of our array. Specifically, we numerically compute the components of the acoustic radiation force (ARF) on the filament by means of momentum flux integration over a closed surface surrounding the levitated object [33]. These simulations were performed in 2D for two separate planes of interest (Fig. 2a): the circular cross-section of the cylindrical array (x-y plane) and the length of the array (y-z plane). Initially, we focus on simulations in two dimensions as these offer a balance between the model accuracy and computation time. Subsequently, we validate the stabilizing behavior in full 3D finite element simulations. In our model, we vary the position of the soft-material filament (PLA) throughout the array in the x-y plane to establish the trap location, radiation force magnitude, and optimal array diameter. On

the other hand, analysis over the y-z plane allows us to evaluate optimal transducer spacing along the length of the cylindrical array. Combining the results from both planes informs the optimal geometry of the proposed levitation array to support the filament during extrusion.

130131

126

127

128

129

RESULTS

132

133

134

135

136

137

138

139

140

141

142

143

144

145

146

147

We design an extended cylindrical array to achieve linear contactless support. The choice of array shape was selected to establish stable levitation of the filament from all sides along the length of extrusion. The proposed array was evaluated for maximum acoustic radiation force while maintaining an evenly distributed force over the surface of the filament. The cross-sectional profile of the array will determine the magnitude of applied radiation force and its selection will depend on the output acoustic frequency and the profile/diameter of the individual acoustic transducers. We note that increasing the radius of the cylindrical array allows more transducers to be placed along the circumference of the array but can reduce the applied radiative force from each individual transducer due to an increasing distance between the levitated object and the sources of pressure. In our analysis, we found that by selecting a radius of 45 mm, we can maintain a high acoustic radiation force while minimizing the total number of necessary transducers. To simplify the integration of the acoustic array and a 3D printer, we removed several transducers from the circumference of the array, as seen in Fig. 2a (also VIDEOS 1 and 2), therefore creating a gap (40 mm) that allows a nozzle to reach

into the intended acoustic trap. **Fig. 2b** shows the cross-sectional profile of the array and the corresponding acoustic field profile obtained in COMSOL Multiphysics.

150

151

152

153

154

155

156

157

158

159

160

161

162

163

164

165

166

167

168

169

149

148

To determine the ranges of filament size and output pressure for which stable support can be achieved, we varied the filament radius and harmonic output pressure and recorded the resulting acoustic radiation force. We then examined how this radiation force compares to the force of gravity on PLA filament (density of 1.25 g/cm³), a commonly used material in FFF (fused filament fabrication) printing. Fig. 2c shows the numerically established relationship between the radiation force and the gravitational force on the filament. We observe that low output pressures are unable to provide sufficient contactless support (i.e., the force of gravity is greater than the acoustic force); however, as the output pressure increases, a regime of potential trapping is realized (i.e., the acoustic force is greater than the force of gravity). We assess that a harmonic output pressure of 250 Pa per transducer provides a reasonable estimate for the selected transducers while ensuring a levitation range over the desired nozzle sizes. In the subsequent analysis of trap regions and transducer spacing, we select a filament radius of 0.2 mm (diameter 0.4 mm), which is a common nozzle size used in 3D printing. We determine the optimal locations for filament trapping and the trap size by

numerically analyzing the components of the acoustic force on the filament. To do this, we sweep the position of the filament on the X-Y cross-section plane and record the lateral trapping force (F_x) and the vertical supporting force (F_y) that is antiparallel to gravity (note that Z-axis is the extrusion axis). **Fig. 3a** shows the profile of the vertical

force. We expect that a suitable trapping location would be located along the centerline of the trap at a vertical height between $\frac{\lambda}{8}$ and $\frac{\lambda}{4}$ from the center of the array. We observe the maximum value of F_y is achieved along the x=0 line, which indicates that the filament would be supported near these coordinates. To assess whether there is sufficient lateral/horizontal force, we refer to **Fig. 3b**, which depicts F_x as a function of the filament position. Indeed, we observe that the profile of the lateral force is stabilizing – that is, $F_x>0$ for x<0 and $F_x<0$ for x>0. By evaluating the radiation force exerted on filament at different positions throughout the array, we also observe the overall size of the acoustic trap, which extends approximately 2 mm in either direction horizontally and 1 mm in either direction vertically. A larger trap size is key to the success of supporting the filament during extrusion as it allows for increased tolerance in the nozzle placement. Specifically, this enables for off-center extrusion to be corrected and fully supported without recalibration of the printing device.

Optimal Transducer Arrangement

In addition to creating a sufficient trapping region for the nozzle, a successful continuous extrusion of filament requires an evenly distributed acoustic radiation force. The arrangement and spacing between source elements in the array translates directly into the strength and the uniformity of the acoustic radiation force. By evaluating different transducer spacings, we assess an optimal range of locations in which transducers can be placed to create an effective linear trap. Transducer spacing ranging from 0 mm to 5 mm were investigated, and the force trends are shown in **Fig. 4a**. We

194

195

196

197

198

199

200

201

202

203

204

205

206

207

208

209

210

211

212

213

observe that the acoustic force remains positive and relatively uniform for spacings up to approximately 4 mm. The relative uniformity of the force along the length of the array is attributed to enhanced interference between sources in the array. Beyond this region, nodal acoustic traps begin to form along the z-axis. Low-pressure regions exist between these nodes, causing the filament to experience a downward acoustic force as seen in Fig. 4c. A general feature of these nodal traps is that they can support levitation of isolated spherical subwavelength objects. However, when it comes to supporting an elongated object such as an extruding filament, these nodal traps are detrimental as they do not provide a positive force along the entire length of the filament. Based on this analysis, we chose a spacing of 3 mm for the synthesized array, as seen in Fig. 4b. This spacing provides a relatively uniform force distribution while increasing the length of the array and, in turn, allowing longer filament lengths to be printed for a given number of transducers. We comment that the forces observed in Fig. 4 are primarily used to display the trends that develop as transducer spacing increases; the overall magnitude of the force is not relevant for analyzing the trends.

The presented numerical modeling of the trapping system is useful for iterative design of the filament support geometry; however, there is a potential for such simplified 2D analysis to ignore the coupling effects and the effects due to the finite size of the system that can only be modeled in a three-dimensional space. To develop a more realistic understanding of the acoustic force on the linear filament, we analyze the trapping performance in full 3D finite element acoustic simulations. Since such

simulations are computationally demanding and long, we primarily use them to validate the hypothesis that the linear filament will be stably supported during extrusion.

We model the established array geometry in three dimensions and evaluate each component of the acoustic radiation force $(F_{x,y,z})$ over the surface a cylinder of extruded filament with a standard diameter of 0.4 mm and length of 40 mm. We then vary the filament location along the lateral direction (x-axis) to assess the size and location of the acoustic trap, as seen in **Fig. 5.** We determine the radiation force on a cylinder of filament at the same vertical position as before. Importantly, we observe a restorative lateral force which increases until the filament reaches an offset of $x \approx 2.2$ mm, or roughly $\lambda/4$, thus creating a stable trap capable of supporting larger filament diameters and allowing for slight misalignment of the extrusion nozzle. We note that numerical simulation in three dimensions results in a more conservative estimate of acoustic radiation force; in practice, this can be remedied by increasing the transducer output pressure if necessary.

Experimental Demonstration

Having established a suitable geometry and arrangement of acoustic sources, we proceed to build a concept prototype and test its ability to support and stabilize the filament during extrusion. First, to test the predictions of our numerical finite element simulations, we successfully levitated a single strand of pre-extruded PLA filament with a diameter of 0.4 mm in the array. We then proceed to examine the effects of contactless acoustic support on 3D printing extrusion. We focused on printing the material in a way that prevents over-extrusion while minimizing tension in the extruded

filament. This step was taken to ensure our results were minimally impacted by the experimental setup. In our tests, the extrusion is initiated from a vertical base positioned on the beginning end of the array. Fig. 6a shows a line of filament being extruded over time when the transducer array is turned off as a control case. Fig. 6b shows extrusion when the transducer array is turned on. Full videos of each print can be found in the Supplementary Materials (VIDEO 1 corresponds to the case when the acoustic field is "off"; in VIDEO 2, the field is turned "on" to engage acoustic force support). We observe a clear advantage of supporting the filament during extrusion: without the air bed support, the filament sags down appreciably; in contrast, when the air bed is present, there is a significantly smaller deviation in the vertical position of the filament. Additional analysis and comparison of filaments of different diameters during extrusion (with fields "off" and fields "on") is presented in the Supplementary Materials. In all cases, we observe that the presence of acoustic fields has a significant impact on stabilizing the extruded PLA filament.

We remark that this is intended as a prototype concept demonstration: further improvement in acoustic field profile and printing conditions would help improve the quality and stability of extrusion. For example, the extrusion on the acoustic air bed is noticeably more uniform in the second half (center and the right segments) of the array. We suspect this arises from the lack of uniformity of the acoustic field due to intrinsic (and, at times, large) transducer-to-transducer variation. It should also be noted that, for simplicity, our simulations do not account for the presence of the nozzle and the extrusion head, which could lead to discrepancies between the theory and the

experiment. Additionally, it was assumed that all transducers have the same phase and pressure output when driven by an identical signal, an assumption that may not always hold in a real system and could affect the performance of the air bed support during extrusion. For future work, we believe that the best-performing support will be realized with an array of individually addressable transducers where the shape and intensity of trapping can be spatially altered in a dynamic fashion.

SUMMARY

In summary, we analyzed the dynamics of soft-material extrusion in the presence of a linear acoustic radiation force profile as a method for contactless support in linear additive manufacturing. By introducing a tailored acoustic potential, we demonstrate that a commonly used 3D material filament can be supported during extrusion in a prototype device that integrates a commercial 3D printer with user control code. Optimal system geometry and acoustic source arrangements are studied through finite-element acoustic simulations. This device expands upon previous works on acoustic trapping by investigating the conditions for and realizing uniformly distributed linear acoustic potentials suitable for material extrusion and investigating the filament behavior in the acoustic field.

We envision several directions for future work. One possibility is to extend the numerical analysis to full 3D finite element simulations, which would improve the fidelity of the physical model, result in more optimal device designs and transducer configurations, and improve the uniformity of printing. Another possibility is to explore single-sided levitation configurations, rather than the double-sided transducer

Vibrations and Acoustics

arrangement investigated in this work, which could allow for a wider range of object shapes and sizes that could be supported during printing. In addition, incorporating arrays of individually digitally addressable transducers could enable the synthesis of complex acoustic potentials to support extrusion along multiple directions. Investigating the interaction between actively reconfigurable, time-dependent acoustic potentials and the thermo-mechanical dynamics of material extrusion is also a relevant direction for future research. The concept of 3D printing on an air bed could potentially lead to fewer surface defects, reduced material waste, cost, and manufacturing time associated with the generation of solid supports in conventional 3D printing.

FUNDING

The authors acknowledge support from the Air Force Office of Scientific Research (AFOSR) under Grant No. FA9550-22-1- 0070. This material is based upon work supported by the National Science Foundation under Grant No. 2318094.

REFERENCES

299 [1] Bruus, H., 2012, "Acoustofluidics 7: The Acoustic Radiation Force on Small Particles," Lab Chip, **12**(6), pp. 1014–1021.

301

298

302 [2] Settnes, M., and Bruus, H., 2012, "Forces Acting on a Small Particle in an Acoustical 303 Field in a Viscous Fluid," Phys. Rev. E Stat. Nonlin. Soft Matter Phys., **85**(1 Pt 2), p. 304 016327.

305

306 [3] Andrade, M. A. B., Bernassau, A. L., and Adamowski, J. C., 2016, "Acoustic Levitation of a Large Solid Sphere," Appl. Phys. Lett., **109**(4), p. 044101.

308

Glynne-Jones, P., Mishra, P. P., Boltryk, R. J., and Hill, M., 2013, "Efficient Finite Element Modeling of Radiation Forces on Elastic Particles of Arbitrary Size and Geometry," J. Acoust. Soc. Am., **133**(4), pp. 1885–1893.

312

5] Cummer, S. A., Christensen, J., and Alù, A., 2016, "Controlling Sound with Acoustic Metamaterials," Nature Reviews Materials, 1(3), pp. 1–13.

315

316 [6] Shi, Q., Di, W., Dong, D., Yap, L. W., Li, L., Zang, D., and Cheng, W., 2019, "A General Approach to Free-Standing Nanoassemblies via Acoustic Levitation Self-Assembly," ACS Nano, **13**(5), pp. 5243–5250.

319

320 [7] Marzo, A., Barnes, A., and Drinkwater, B. W., 2017, "TinyLev: A Multi-Emitter Single-Axis Acoustic Levitator," Rev. Sci. Instrum., **88**(8), p. 085105.

322

323 [8] Marzo, A., Corkett, T., and Drinkwater, B. W., 2018, "Ultraino: An Open Phased-324 Array System for Narrowband Airborne Ultrasound Transmission," IEEE Trans. 325 Ultrason. Ferroelectr. Freq. Control, **65**(1), pp. 102–111.

326

[9] Marzo, A., Seah, S. A., Drinkwater, B. W., Sahoo, D. R., Long, B., and Subramanian,
 S., 2015, "Holographic Acoustic Elements for Manipulation of Levitated Objects,"
 Nat. Commun., 6, p. 8661.

330

331 [10] Vandaele, V., Lambert, P., and Delchambre, A., 2005, "Non-Contact Handling in Microassembly: Acoustical Levitation," Precis. Eng., **29**(4), pp. 491–505.

333

[11] Wu, H., Zhu, J., Wang, X., and Li, Y., 2021, "Design of Ultrasonic Standing Wave
 Levitation Support for Three-Dimensional Printed Filaments," J. Acoust. Soc. Am.,
 149(4), p. 2848.

337

Trinh, E. H., 1985, "Compact Acoustic Levitation Device for Studies in Fluid Dynamics and Material Science in the Laboratory and Microgravity," Rev. Sci. Instrum., **56**(11), pp. 2059–2065.

342	[13]	Andrade, M. A. B., Okina, F. T. A., Bernassau, A. L., and Adamowski, J. C., 2017,
343		"Acoustic Levitation of an Object Larger than the Acoustic Wavelength," J. Acoust.
344		Soc. Am., 141 (6), p. 4148.
345		
346	[14]	Kandemir, M. H., and Çalışkan, M., 2016, "Standing Wave Acoustic Levitation on an
347		Annular Plate," J. Sound Vib., 382 , pp. 227–237.
348		
349	[15]	Zhao, S., and Wallaschek, J., 2011, "A Standing Wave Acoustic Levitation System for
350		Large Planar Objects," Arch. Appl. Mech., 81(2), pp. 123–139.
351		
352	[16]	Baresch, D., Thomas, JL., and Marchiano, R., 2016, "Observation of a Single-Beam
353		Gradient Force Acoustical Trap for Elastic Particles: Acoustical Tweezers," Phys.
354		Rev. Lett., 116 (2), p. 024301.
355		
356	[17]	Xie, W. J., Cao, C. D., Lü, Y. J., Hong, Z. Y., and Wei, B., 2006, "Acoustic Method for
357		Levitation of Small Living Animals," Appl. Phys. Lett., 89 (21), p. 214102.
358		
359	[18]	Priego-Capote, F., and de Castro, L., 2006, "Ultrasound-Assisted Levitation: Lab-on-
360		a-Drop," Trends Analyt. Chem., 25 (9), pp. 856–867.
361		
362	[19]	Watanabe, A., Hasegawa, K., and Abe, Y., 2018, "Contactless Fluid Manipulation in
363		Air: Droplet Coalescence and Active Mixing by Acoustic Levitation," Sci. Rep., 8(1),
364		p. 10221.
365		
366	[20]	Foresti, D., Nabavi, M., Klingauf, M., Ferrari, A., and Poulikakos, D., 2013,
367		"Acoustophoretic Contactless Transport and Handling of Matter in Air,"
368		Proceedings of the National Academy of Sciences, 110 (31), pp. 12549–12554.
369		
370	[21]	Nikolaeva, A. V., Sapozhnikov, O. A., and Bailey, M. R., 2016, "Acoustic Radiation
371		Force of a Quasi-Gaussian Beam on an Elastic Sphere in a Fluid," IEEE Int Ultrason
372		Symp, 2016 .
373		
374	[22]	Xie, W. J., and Wei, B., 2001, "Parametric Study of Single-Axis Acoustic Levitation,"
375		Appl. Phys. Lett., 79 (6), pp. 881–883.
376		
377	[23]	Baresch, D., and Garbin, V., 2020, "Acoustic Trapping of Microbubbles in Complex
378		Environments and Controlled Payload Release," Proc. Natl. Acad. Sci. U. S. A.,
379		117 (27), pp. 15490–15496.
380	_	
381	[24]	Santesson, S., and Nilsson, S., 2004, "Airborne Chemistry: Acoustic Levitation in
382		Chemical Analysis," Anal. Bioanal. Chem., 378(7), pp. 1704–1709.
383		
384	[25]	Fzcurdia I Morales R Andrade M A B and Marzo A 2022 "LeviPrint:

Contactless Fabrication Using Full Acoustic Trapping of Elongated Parts," ACM

386 387 388	SIGGRAPH 2022 Conference Proceedings, Association for Computing Machinery, New York, NY, USA, pp. 1–9.
	Foresti, D., Bjelobrk, N., Nabavi, M., and Poulikakos, D., 2011, "Investigation of a Line-Focused Acoustic Levitation for Contactless Transport of Particles," J. Appl. Phys., 109 (9), p. 093503.
	Andrade, M. A. B., Pérez, N., and Adamowski, J. C., 2018, "Review of Progress in Acoustic Levitation," Braz. J. Phys., 48 (2), pp. 190–213.
	Xie, W. J., and Wei, B., 2003, "Temperature Dependence of Single-Axis Acoustic Levitation," J. Appl. Phys., 93 (5), pp. 3016–3021.
	Andrade, M. A. B., Ramos, T. S., Okina, F. T. A., and Adamowski, J. C., 2014, "Nonlinear Characterization of a Single-Axis Acoustic Levitator," Rev. Sci. Instrum., 85 (4), p. 045125.
	Morris, R. H., Dye, E. R., Docker, P., and Newton, M. I., 2019, "Beyond the Langevin Horn: Transducer Arrays for the Acoustic Levitation of Liquid Drops," Phys. Fluids, 31 (10), p. 101301.
	Xie, W. J., and Wei, B., 2002, "Dependence of Acoustic Levitation Capabilities on Geometric Parameters," Phys. Rev. E Stat. Nonlin. Soft Matter Phys., 66 (2 Pt 2), p. 026605.
	Karlsen, J. T., and Bruus, H., 2015, "Forces Acting on a Small Particle in an Acoustical Field in a Thermoviscous Fluid," Physical Review E, 92 (4).
414 [33 415 416	Stein, M., Keller, S., Luo, Y., and Ilic, O., 2022, "Shaping Contactless Radiation Forces through Anomalous Acoustic Scattering," Nature Communications, 13 (1).

Figure Captions List

- Fig. 1 Contactless 3D printing via material extrusion on an acoustic air bed. Concept schematic of directing a tailored acoustic wavefront to contactlessly support material during extrusion. Engineered arrangement of transducers induces an acoustic radiative force (\vec{F}_{arf}) capable of counteracting the force of gravity (\vec{F}_{g}) and spatially stabilizing the extruded material in the acoustic potential.
- Fig. 2 Numerical finite-element acoustic model and analysis of the acoustic radiation force. (a) Model of the source array as used experimentally (see Videos 1 and 2). (b) Cross-section of the transducer array and the resulting acoustic field profile. The Y-axis denotes gravity (gravity points along -Y) and the Z-axis is the extrusion direction (out of plane). Black circle denotes the integration boundary for evaluating the radiation force on the filament. (c) Vertical acoustic force (F_y) and the gravitational force (F_g) as a function of the filament radius and the output transducer pressure. A functional region in which applied radiative force is greater than the force of gravity is established for the specified array geometry in (a).
- Fig. 3 Analysis of acoustic force components that support the filament. (a) Vertical radiation force (F_y) exerted on the circular filament cross section. (b) Horizontal force (F_x) exerted on the filament. The filament is extruded along the Z-axis; gravity points in the -Y direction. The magnitude of

applied acoustic radiation force is shown along with the filament trapping location. Vertical force is significantly greater than horizontal force to ensure stable support against the gravitational force on the filament.

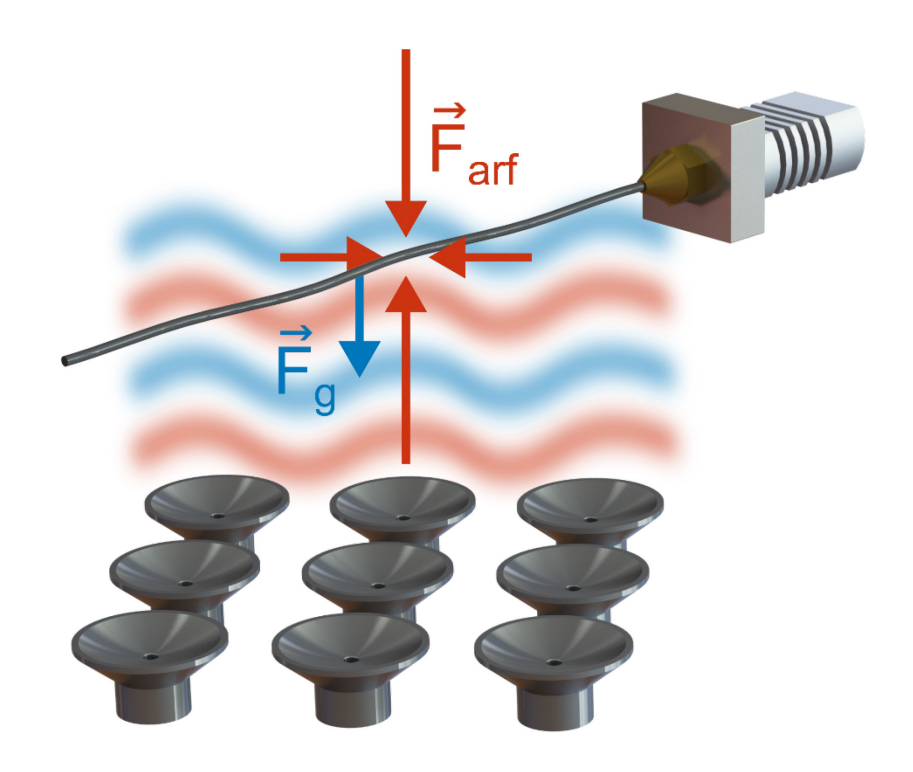
- Fig. 4 Analysis of optimal transducer array arrangement during extrusion. Vertical acoustic radiation force (F_y) as a function of position on the plane comprising the extrusion direction (Z) and the gravity direction (-Y). (a) Transducer spacing is 1 mm; (b) Transducer spacing is 3 mm; (c) Transducer spacing is 5 mm. When transducer spacing is increased, the vertical acoustic force F_y becomes weaker and less uniform along the extrusion direction (Z), even turning negative in some locations along the filament. The displayed trend points to an optimal tradeoff between force uniformity/magnitude and transducer density.
- Fig. 5 Analysis of contactless material support in three dimensions. Horizontal (lateral) acoustic radiation force (F_x) as a function of horizontal position (x-axis) where x=0 is the stable equilibrium position. Filament diameter is 0.4 mm and total length is 40 mm. Extruded filament will experience a restorative lateral force (F_x) if offset relative to the equilibrium position.
- Fig. 6 Experimental dynamics of extrusion of a 3D-printer filament. (a) Acoustic field is turned OFF, and the filament sags under its weight as it is extruded.

 See also Video 1; (b) Acoustic field is turned ON; the filament is supported by an air bed and better maintains its shape. See also Video 2. The acoustic

Vibrations and Acoustics

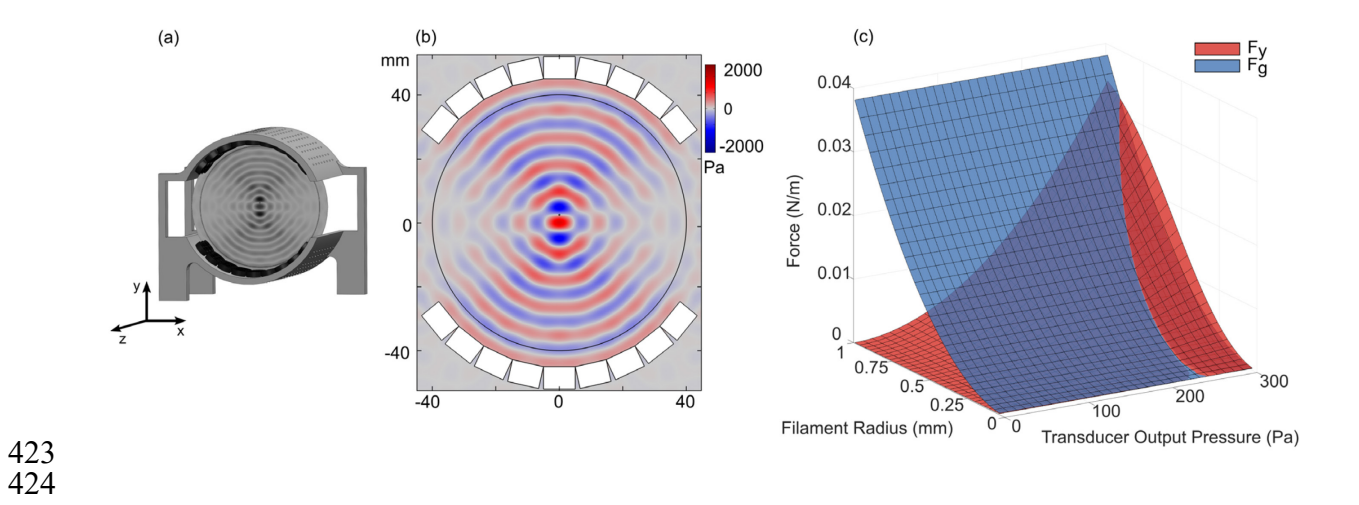
radiation force improves the shape of printing without the need of physical solid supports. The horizontal axis denotes snapshots at different times.

419



421 422 (REVISED)

Vibrations and Acoustics



21

Vibrations and Acoustics

